NASA Technical Memorandum 82901

Use of Fiber-Like Materials to Augment Cycle Life of Thick Thermoprotective Seal Coatings

R. C. Hendricks and G. McDonald
Lewis Research Center
Cleveland, Ohio

August 1982

NASA

USE OF FIBER LIKE MATERIALS TO AUGMENT CYCLE LIFE OF THICK THERMOPROTECTIVE SEAL COATINGS*

R. C. Hendricks and G. McDonald

National Aeronautics and Space Administration
Lewis Research Center
Cleveland Ohio 44135

SUMMARY

Some experimental and analytical studies of plasma sprayed ZrO_2-Y_2O_3 thick seal thermoprotective materials over NiCrAlY bond coats with testing to 1040° C in a Mach 0.3 burner flame are reviewed. These results indicate the need for material to have both compliance and sufficient strength to function successfully as a thick thermoprotective seal material. Fibrous materials may satisfy many of these requirements. A preliminary analysis simulating the simplified behavior of a 25 mm cylindrical SiO_2-fiber material and a 12 mm cylindrical ZrO_2-fiber material indicated significant radial temperature gradients, a relatively cool interface and generally acceptable stresses over the initial portion of the thermal cycle. Subsequent testing of these fiberlike materials in a Mach 0.3 Jet A/air burner flame comfirmed these results.

E-1284

INTRODUCTION

Thermal protective ceramic coatings placed on an internally cooled metal component of a gas turbine have been proposed for some considerable time as a means of operation of heat engines at higher temperature (refs. 1 to 4). Alternately, use of such a coating can conceivably increase the lifetime of highly stressed engine components by permitting operation at equivalent gas temperature and thermodynamic efficiency but at lower component temperature.

Application of thermal protective coatings to some heat engine components has been achieved but successful application of such coatings to the design of critical parts of turbine vanes, blades and seals has remained more of a promise than a reality since reliable prediction of durability or experimental consistency of performance has not been achieved (refs. 3 to 6).

Previous experimental and analytical work (refs. 5 to 9) has shown that thin (0.38 mm) ZrO_2-Y_2O_3 ceramic coatings plasma sprayed on a metal substrate fail after varying lengths of time when cyclically heated by exposure to a 0.3 Mach flame. The location of failure of the ZrO_2-Y_2O_3 is principally in the ceramic in a plane parallel to and within only a few thousands of mm of the ceramic/metal interface.

Observations and measurements from several experiments correlate with the results obtained from the thermal cycling. The principal results include the following items.

*Material previously presented at the International Conference on Metallurgical Coatings and Process Technology sponsored by the American Vacuum Society, San Diego, California, April 4-9, 1982.

1. If a series of specimens with coating thickness varying from 0.38 to 1.14 mm (0.015 to 0.045 in.) are thermally cycled (ref. 4) in the 0.3 Mach flame, there is a strong inverse correlation between coating thickness and coating life. A 1.15 mm coating will spall in one cycle. A 0.38 mm coating will last an average of hundreds of cycles and a 0.13 mm coating has very extended life.

2. When 0.38 mm ZrO_2-YO_3 plasma sprayed coatings are removed by pulling in tension, then both the position of failure and the appearance of the failed surface is identical to the failure of the ceramic in thermal cycling (ref. 6). This suggests that the same method of failure may be occuring in both experiments. In addition the scatter of values for a score of measurements in both cycling and tension have similar distributions.

3. Thermal cycling of ZrO_2-Y_2O_3 coated flat disk surface ("piston head") (unpublished data from G. McDonald) to 1040° C at the specimen center, with the edge temperature approximately 100° C higher, showed repeatedly that separation of the ceramic occurred only in the central region of the plate.

4. ZrO_2 changes structure between ambient and 1040° C where the flame exposure tests were made. In the experiments described here the ZrO_2 had added Y_2O_3 to stabilize the coating against phase change. X-ray measurements of pre- and post-cycled plasma sprayed ZrO_2-Y_2O_3 coatings did not indicate any change in the structure of the ZrO_2 (ref. 7).

5. Specimens cycled at reduced heating rate to tempertures of 900° C have coating lifetimes of over 25 times those cycled at a higher heating rate to temperature of 980° C (ref. 8).

The above results suggest that strong consideration should be given to the thermal-mechanical effects. In this paper we will review sources of stress and investigate methods and materials to minimize detrimental stress effects.

ACKNOWLEDGEMENT

The authors wish to thank John H. Ainsworth, Bethleham Steel Corp., Bethleham, PA 18016, Blake A. Emmerich, Zircar Products, Florida, NY 10921 and R. Dotts, NASA Johnson Space Center, Houston TX, for their assistance in this project.

SOME SOURCES OF STRESS

1. Stress from fabrication

Conventionally the ZrO_2 coatings, due to the extremely high melting temperature of above 2500° C, are plasma sprayed onto the metal substrate. The plasma from the torch, which impinges on the substrate being sprayed, has a high heat transfer rate. For carefully controlled fabrication in which the maximum substrate temperature is held to approximately 200° C, the residual stress at ambient resulting from differential thermal contraction from final temperature of plasma spraying is minimized (ref. 10) but does exist.

2. Stress from heat transfer

a. Free standing ceramic

Spalling within ceramic may be caused by initial heat up when a nonlinear temperature distribution exists across the ceramic. Under these conditions when a safe heat-up rate is exceeded a crack can occur within the

ceramic (ref. 11). The Kienow relation, as expanded by Ainsworth (ref. 12) states that subsurface cracks are caused by changes in curvature due to excessive heating rates and brick geometry

$$\frac{\sigma}{E} = \frac{(d^2T/dz^2)\alpha t^2}{[16 + 3(t/z)^3]}$$

where d^2T/dz^2 represents the tranisent heating rate, α is thermal expansion coefficient, t is the brick thickness and z is the distance behind the hot face. σ/E is the fracture strain. This is the pattern of failure of the ceramic coatings plasma sprayed onto metal substrates when the ceramics are heated as previously described (refs. 5 to 8). Calculations indicate that while this does contribute to the stress, the magnitude is too low to cause failure.

b. Ceramic attached to substrate

When the ceramic coating is either heated or cooled, a thermal gradient is produced in the ceramic which is proportional to the heat transfer rate and the thickness of the coating. A simplified parametric form can be used to estimate the stress, (refs. 5 and 8)

$$\frac{\sigma}{E} = \left[\frac{\alpha}{k(1 - \nu)}\right]\left[\frac{t^2}{d}\right]\left[h\ (T_o - T_s)\right]$$

where α is the difference in thermal expansion coefficient, E is Youngs modulus, k is thermal conductivity, h is heat transfer coefficient, T_o is free stream temperature, T_s is time dependent surface temperature, d is diameter of the cylinder and ν poisson ratio. For a coating thickness of 0.38 mm and a heat transfer of 550 kW/m^2 (0.3 Mach flame) the stress in the coating is 4.4 MPa.

3. Stress from inelastic behavior

Above 980° C (1800° F) ZrO_2 becomes increasingly plastic and if the ceramic coated metal substrate is held at temperatures above 980° C (1800° F) for time sufficient for plastic flow of the ZrO_2 to occur (refs. 12 to 14), then a stretching of the ZrO_2 coating will occur because of the thermal expansion of the metal substrate is greater than the expansion of the ZrO_2. On return to ambient temperature the ceramic is compressively stressed.

Below a temperature of 980° C (1800° F), there is probably insignificant plastic flow of the ZrO_2. For example, 0.038 mm ZrO_2-Y_2O_3 coatings cycled in a 0.3 Mach flame to equilibrium temperature below 980° C (1800° F) have very long life. The increasingly more rapid failure of coatings when cycled to temperature increasingly higher than 1040° C (1900° F) is consistent with increased plastic flow in tension of the ZrO_2 when held at temperatures greater than 980° C (1800° F). This plastic flow increases the compressive stress on the coating when the specimen is returned to ambient.

If the ZrO_2 coating is held at 1040° C (1900° F) long enough to achieve stress relaxation plastic flow, then the strain is (ref. 14)

$$\epsilon_{cr} = NC_o\tau^{0.55}$$

where N represents the number of cycles, Co an empirically determined parameter and τ the time under load. It is assumed that τ is short compared to the time required for complete stress relaxation. On return to ambient this plastic flow produces an additional compressive stress increment which results in an increment in:

$$\sigma_{cr} = 2E\left(\frac{t}{d}\right) NC_o \tau^{0.55}$$

Since there is little control over the stresses which originate in fabrication or conditions of use, it is evident that a compliant coating is required to accommodate stress.

ANALYSIS

Thermal-Stress

Numerical thermal-stress calculations were carried out using the SINDA-FEATS codes (ref. 15 and private communications from G Cowgill and P. Manos of NASA Lewis) for cylinders fabricated from the silica-fiber (SiO_2) and zircona-fiber (ZrO_2) materials and cemented onto metal restraining pins, see sketch in figure 1. The temperature profiles for three thermoprotective materials SiO_2, ZFB and YSZ with thermal diffusivities of 0.17, 0.031, and 0.043 respectively, are illustrated at 0.001 hours into the heating cycle in figure 1. The model is 12 mm in diameter with a 3 mm diameter pin simulating the specimens to be tested. At this time in the cycle, the profiles reflect the competing effects of thermal diffusivity (a) and heat sink capacity (ρc), 0.022, 0.072 and 0.056 for SiO_2, ZFB, and YSZ respectively. The normalized radial and longitudinal stresses resulting from these temperature profiles are illustrated in figure 2. The circumferential stresses are similar to the longitudinal stresses. The radial stress normalization parameter ($E\alpha(\Delta T= 1)$) is 1.45E-5, 1.72E-3, and 1.93E-1 and the longitudinal values are 5.2E-5, 2.9E-3, and 1.93E-1 for SiO_2, ZFB, and YSZ respectively. Each material parameter differs approximately two orders of magnitude. The thermal effects on the SiO_2 material are most pronounced, but the resulting stresses are very small due to the low value of ($E\alpha(\Delta T=1)$). And although the thermal effects are weakest for the YSZ material, the stresses are excessive, due to the high value of ($E\alpha(\Delta T=1)$) The calculated stresses for the fiber materials are, but of course their strength is also low. For the configuration to be tested, the silica-fiber (SiO_2) stresses are 'safe' while the zirconium fiber material (ZrO_2 at 0.5 g/cc) is marginal. The plasma sprayed zirconium (YSZ) stresses are too high, and will not be tested.

Crack Initiation and Arrest

Homogeneous Materials

In addition to the thermal stress factors cited above, both fracture initiation or nucleation and also crack arrest, as discussed for example in references 16 to 19, must be considered. To avoid initiation or nucleation of a crack which is highly dependent on heating and/or cooling rates and

material thermophysical properties, the parameter

$$R^{+} = \frac{k\sigma(1-\nu)s}{hE\alpha}$$

should be maximized, and for crack arrest, the parameter

$$R^{++} = \frac{K\gamma S}{\sigma^2(1-\nu)}$$

should be maximized. The additional parameters are, σ stress, γ surface fracture energy, and S a geometric shape factor.

In developing these parameters, the total elastic energy stored at fracture was equated to the total surface energy required to propagate cracks; for a sphere these relations become (ref. 16),

$$M\gamma A = \frac{\pi\sigma^2(1-\nu)d^3}{28\,E}$$

and the calcuated crack area becomes,

$$A_{calc} = \frac{\pi\sigma^2(1-\nu)d^3}{28\,ME\,\gamma}$$

where M is the number of cracks. When $A_{calc} > \pi d^2/4$, the sphere will fail (gaping crack equivalent).

It should be recognized that these relations are general material parameters.

Now consider the application of these parameters to the fracture resistance of a series of materials. For example, a hardened red hot steel sphere shatters when quenched in an oil bath (private communication from J. Padovan). Applying the above relations to the hardened sphere, assuming M = 5 (ref. 16)

$$A_{calc} = \frac{\pi(2.5\times10^5\times6.9\times10^4)\ (1-.25)\left(\frac{2.54}{3}\right)^3}{27\times5\times29\times10^6\times6.9\times10^4\times10^5} = 6.6\text{cm}$$

$$A_{calc} = \frac{\pi d^2}{4} = \frac{\pi}{4}\left(\frac{2.54}{4}\right)^2 = 0.3\text{cm}^2$$

and hence the sphere should, and does, fail (i.e., resistance to crack nucleation is small* and resistance to propagation is insufficient to arrest crack propagation). However, if a lower strength steel had been used, such as mild steel,

---

$$*R = \frac{(10)\ (280\ 000)\ (1-.3)}{5\times10^3\times29\times10^6\times8\times10^{-6}} \sim 2$$

$$A_{calc} = (6.6)\left(\frac{20}{250}\right)^2 = 0.04 \text{ cm}^2 < \frac{\pi d^2}{4} = A$$

indicating the sphere should not, and did not, fail**.

Similar examples for spheres of different materials are included in the table.

Material	A calc	A	Failure	Ref.
Porcelain	1000	20	yes	19
Fireclay body	4	20	no	19
Alumina reinforced Molybdenum fibers	0.012	20	no	19
Hardened steel	6	0.3	yes	23
Mild steel	0.04	0.3	no	23

The generality of these parametric relations provides a basis for their application to coatings, where it is desired to avoid catastrophic failures due to unarrested crack propagation.

Multi-layer Materials

While some criteria exists for cracking of homogeneous materials, special consideration needs to be given to multiple materials as TPC.

If one considers two types of flaws, parallel and perpendicular to the surface a compression load parallel to the surface and a tensile load normal to the surface would open a parallel flaw and tend to close a perpendicular flaw. Conversely, a tensile load parallel to the surface and a compressive load normal to the surface would close a flaw parallel to the surface and tend to open a perpendicular flaw. As the NiCrAlY-YSZ interface is quite irregular with a type of mechanical-chemical diffusion bond, there are 'periodic' parallel and perpendicular flaws. These flaws respond to thermal cycling in such a way that short perpendicular cracks that do not penetrate the surface or interface could be beneficial, except for oxidation, and the parallel cracks detrimental. As the parallel cracks propagate the surface will tend to 'peel' off leaving nircrally tips and YSZ valleys.

For a 0.4 mm coating on a 13 mm diameter cylinder, the longitudinal and circumferential stresses are nearly the same. The implication being that penetration and propagation of longitudinal and/or circumferential surface cracks appears equally probable. Upon cooling, tensile loading can propagate critical flaws through the surface to form gaping flaws. Under intense aerothermomechanical loading and a weakened surface, these flaws can continue to propagate.

**For the same conditions, resistance to nucleation decreases by an order of magnitude, but resistance to propagation increases by two orders of magnitude.

From data obtained from bending of YSZ-NiCrAlY on 0.8 by 38 by 250 mm stainless steel test specimens, adjacent vertical visible gaping cracks can appear at spacings of

$$b = 0.5 + 0.045(t/t^*)^2$$

where $t^* = 0.127$ mm (0.005 in.), t the coating thickness and the fragment width (b) in mm.

The appearance of a vertical gaping crack or combinations (e.g., parallel, H-type) and associated misalinement stresses coupled with the severe aerothermomechanical loading of reheat intensifies parallel crack loading and propagation along with radial stresses. A 'hot spot' develops and often the coating will 'pop' off the specimen leaving the characteristic NiCrAlY tips and YSZ valleys. Miller (privately communicated at NASA Lewis) has taken lapse time motion pictures of coating losses; it appears that coating fragments may be of the order of (b) and larger.

Compliant Fiber Materials

The ratio of the resistance to crack propagation (refs 16 and 17) for the case of the silica fiber board to that of plasma sprayed yittria-stabilized-zirconia (YSZ) becomes

$$y = \frac{R^{++}_{SiO_2}}{R^{++}_{ysz}} = \left(\frac{E_{SiO_2}}{E_{ysz}}\right)\left(\frac{\sigma_{ysz}}{\sigma_{SiO_2}}\right)^2\left[\frac{(1-\nu)_{SiO_2}}{(1-\nu)_{ysz}}\right]\left(\frac{\gamma_{SiO_2}}{\gamma_{ysz}}\right)\left(\frac{S_{SiO_2}}{S_{ysz}}\right)$$

The fracture surface energy has not been established for either the silica fiber board (SiO_2) or the plasma sprayed (YSZ). The best estimates are: $1 < \gamma_{YSZ} < 2$ and $\gamma_{SiO_2} > 10$. Other properties for YSZ are taken from reference 1 and those of the silica fiber board (SiO_2) are taken from reference 19. For these conditions, the ratio becomes (assuming a similar geometric configuration) Y = 135, see table I.

TABLE I. - MATERIAL PROPERTIES USED TO CALCULATE THE Y-PARAMETER (* Estimated)

Material	E, MPa	σ, MPa	ν	γ, MPa-m	S
SiO_2	410	0.48	0.25	10	1
ZrO_2	1.5E3*	0.9*	0.16	10	1
YSZ	47E3	28.2	0.16	2	1

In essence the silica fiber board (SiO_2) is at least two orders of magnitude better at arresting crack propagation than is the plasma sprayed material (YSZ).

Comparing the silica fiber board with the zirconia felt board material (ZFB) is more difficult because properties of the felt board are not well established. To make the comparison, an assumption is made that

$$\left(\frac{E_{ZFB}}{E_{YSZ}}\right)\left(\frac{\sigma_{YSZ}}{\sigma_{ZFB}}\right) = 1$$

with other properties taken from reference 21, and the resistance to crack propagation becomes Y = 138.

Thus, as a first estimate, the silica and the zirconia fiber boards should have a similar tolerance to crack propagation.

EXPERIMENTAL APPARATUS

The 0.3 Mach Jet-A/air burner facility is essentially that described and used in references 4 to 7. The fiber materials were shaped and mounted onto support pins and exposed to the burner flame. The specimens were not rotated and positioned close to the burner to provide a more hostile thermal environment. For each of the two materials, SiO_2(silica fiber board) and ZrO_2 (Zirconium fiber board), a 'square' and a 'round' cylinder were shaped from material billits. These SiO_2 cylinders were nominally 25 mm in diameter (square) and the ZrO_2 cylinders were 12 mm in diameter (square). The SiO_2 specimens were fit over a 12 mm diameter porcelain enamel coated rod which formed a fusion SiO_2/SiO_2-bond after one burner cycle. The ZrO_2 specimens were cemented with a zirconium based cement to ZrO_2-Y_2O_3/NiCrAlY coated 3.2 mm diameter pins.

RESULTS

SiO_2 - Fiber Material

Initial tests with a 'round' sample 25 mm diameter by 150 mm long withstood 10 hours on one side followed by 22 hours when rotated 180 deg. The leading edge temperature estimate was noted at 1090° C (2000° F). The material eroded to some extent. Particles dislodged from the burner may have been responsible for the erosion. No other damage could be found.

A 25 mm square cylinder with an edge turned toward the burner was heated to 1230° C (2250° F) at the edge and about 1040° C (1900° F) only 6 mm away. The material heat shrank and the leading edge became concave, but did not fail in 11 hours of continuous operation.

With the square cylinder reversed, and the temperature reduced to between 1040° and 1090° C (1900° to 2000° F) the edge looked quite good even after 22 hours of continuous operation. Some surface erosion was noted, but at the cooler burner temperatures the material did not apprear to shrink as much. Repeating the test with the fuel/air ratio adjusted to give about 1040° C (1900° F), the sample was cycled approximately 650 times (2 min heat, 1 min cool) without any visible deterioration.

Zirconia Fiber Material

A square cylinder of ZrO_2 fiber board (0.5 g/cc) was tested with the Mach 0.3 flame directed at the flat surface; after three cycles it was noted that a longitudinal crack appeared on the reverse side (opposite the flame heated surface). The visible radiation indicated a white hot face to the flame and a rather cool (nonluminous) surface at the rear central longitudinal part of the cylinder. The sample failed in four cycles.

A round cylinder, prepared in the same manner as the square cylinder, split in plane approximate normal to the pin but did not otherwise fail. Optical temperature measurements indicated that

$$1260^\circ\ C\ (2300^\circ\ F) < T_{front} < 1315^\circ\ C\ (2400^\circ\ F)$$
$$925^\circ\ C\ (1700^\circ\ F) < T_{rear} < 980^\circ\ C\ (1800^\circ\ F)$$

The burner temperature was increased to its maximum. The specimen did not come off the pin and the optical temperatures indicated the following:

$$1370^\circ\ C\ (2500^\circ\ F) < T_{front} < 1430^\circ\ C\ (2600^\circ\ F)$$

These materials are susceptible to particle erosion in the uncoated condition. It should also be pointed out that these materials could also serve as strain isolators (e.g., ref. 1) perhaps enabling the metal isolators to be replaced by a fiber-ceramic material.

SUMMARY OF RESULTS

A significant amount of experimental and theoretical evidence indicates that strong consideration be given to thermal-mechanical effects. Although in many cases there is little control over the conditions causing stresses such as those resulting from fabrication, heat transfer and inelastic behavior, destruction of the coating may be avoided by using a compliant material to accomodate the generated stresses and arrest crack propagation. The analysis and experiments on two compliant fiber board materials, SiO_2 and ZrO_2, show that, while they have low strength, they do withstand the thermal-mechanical and aerodyanmic loadings imposed by a 0.3 Mach Jet A/air burner flame. Further, the ZrO_2 fiber material appears capable of withstanding surface temperatures of over 1400° C (2600° F).

While the fiberlike materials show promise as strain isolators and thermoprotective agents the thicknesses are large and the overall strength is very low for currently available materials. Although the principles have been set forth, the development is incomplete.

Motion pictures are used to further assess the results.

REFERENCES

1. Taylor, C. M.; and Bill, R. C.: Thermal Stresses in a Plasma-Sprayed Ceramic Gas Path Seal. J. Aircr., Vol. 16, No. 4, Apr. 1979, pp. 239-246.

2. Bill, R. C.; Wisander, D. W.; and Brewe, D. E.: Preliminary Study of Methods for Providing Thermal Shock Resistance To Plasma-Sprayed Ceramic Gas-Path Seals. NASA TP-1561, 1980.

3. Levine, Stanley R.; Miller, Robert A.; and Gedwill, Michael A.: Improved Performance Thermal Barrier Coatings. NASA TP, 1981.

4. Wachtman, John, B., Jr.: National Materials Policy: Critical Materials and Opportunities. Am. Ceram. Soc. Bull. 61, No. 2, Feb. 1982, pp. 214-220.

5. McDonald, G.; and Hendricks, R. C.: Effect of Thermal Cycling on ZrO_2-Y_2O_3 Thermal Barrier Coatings. NASA TM-81480, 1980.

6. Hendricks, R. C.; and McDonald, G.: Assessment of Variations in Thermal Cycle Life Data of Thermal Barrier Coated Rods. NASA TM-81743, 1981.

7. Hendricks, R. C.; McDonald, Glen: Effects of Arc Current on the Life in Burner Rig Thermal Cycling of Plasma Sprayed ZrO_2-Y_2O_3. Presented at the 6th Annual Conf. on Composites, (Cocoa Beach FL.), Jan. 17-21 1982.

8. Hendricks, R. C.; and McDonald, G.: Prolonging Thermal Barrier Coated Specimen Life by Thermal Cycle Management. NASA TM-81742, 1981.

9. McDonald, G.; and Hendricks, R. C.: Some Thermal Stress Problems in Porcelain Enamel Coated Rods. Proceedings Porcelain Enamel Institute, Vol. 42, Am. Ceramic Society, 1980, pp. 178-182.

10. Sevcik, William R.; and Stoner, Barry L.: An Analytical Study of Thermal Barrier Coated First Stage Blades in a JT9D Engine. (PWA-5590, Pratt and Whitney Aircraft Group; NASA Contract NAS3-21033.) NASA CR-135360, 1978.

11. Ainsworth, John H.: Calculation of Safe Heat Up Rates for Steel-Plant Furnace Linings. Am. Ceram. Soc. Bull. Vol. 58, No. 7, July 1979, pp. 676-678.

12. Firestone, R.; and Bill, R. C.: Creep Evaluation of Plasma-Sprayed Zirconia Thermal Barrier Coatings. NASA CR167868, 1982.

13. Firestone, R.; Logan, W. R.; Adams, J. W.; and Bill, R. C.: Creep of Plasma-sprayed Jittria-Stabilized Zirconia Thermal Barrier Coatings (48-C-82C). Presented at the 6th Annual Conf. on Composites, sponsored by the American Ceramic Society, Cocoa Beach, Fla., Jan. 17-21, 1982.

14. Hendricks, R. C.; and McDonald, G.: Some Inelastic Effects of Thermal Cycling on ZrO_2-Y_2O_3 Thermal Barrier Coated Rods. Proposed NASA TP, 1981.

15. Swanson, J. A.: FEATS - A Computer Program for the Finite Element Thermal Stress Analysis of Plane or Axisymmetrical Solids. WANL-TME-1888, Westinghouse Electric Corp., 1969.

16. Hasselman, D. P. H.: Elastic Energy at Fracture and Surface Energy as Design Criteria for Thermal Shock. J. Am. Ceram. Soc., Vol 46, No. 11, Nov. 1963, pp 535-540.

17. Ainsworth, J. H.; and Herron, R. H.: Thermal Shock Damage Resistance of Refractories. Am. Ceram. Soc. Bull., Vol 53, No. 7, July 1974, pp. 533-538.

18. Kingery, W. D. ; Bower, H. K.; and Uhlmann, D. R.: Introduction to Ceramics. Second ed. John Wiley a Sons, 1975.

19. Hasselman, D. P. H : Unified Theory of Thermal Shock Fracture Initiation and Crack Propagation in Brittle Ceramics. J. Am. Ceram. Soc., Vol. 52, No. 11, Nov. 1969, pp. 600-604.

20. Buckley, John D; Strouhal, George; and Gangler, James, J: Early Development of Ceramic Fiber Insulation for the Space Shuttle. Am. Ceram. Soc. Bull., Vol. 60, No. 11, 1981, pp. 1197-1199. See also as a general reference: pp. 1180-1195.

21. High Temperature Thermal Insulation, Technical Bulletins, Zircar Products Inc. Florida, NY, 1979.

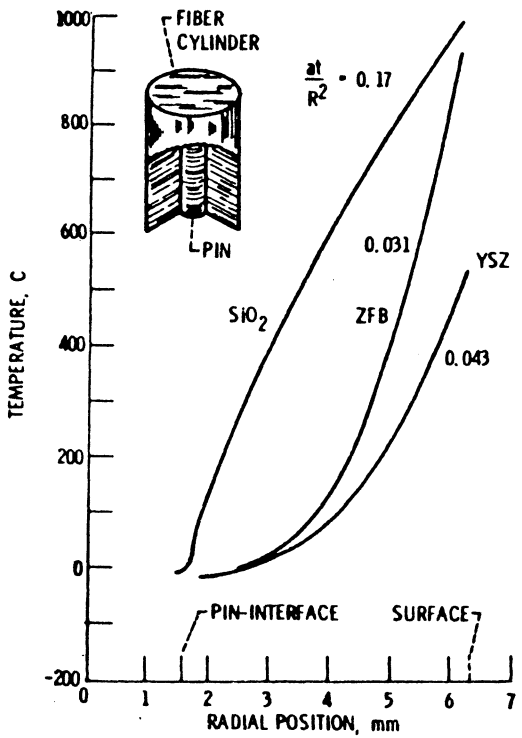

Figure 1. - Radial temperature distribution at 10^{-3} hr into the heating cycle for three thermoprotective materials.

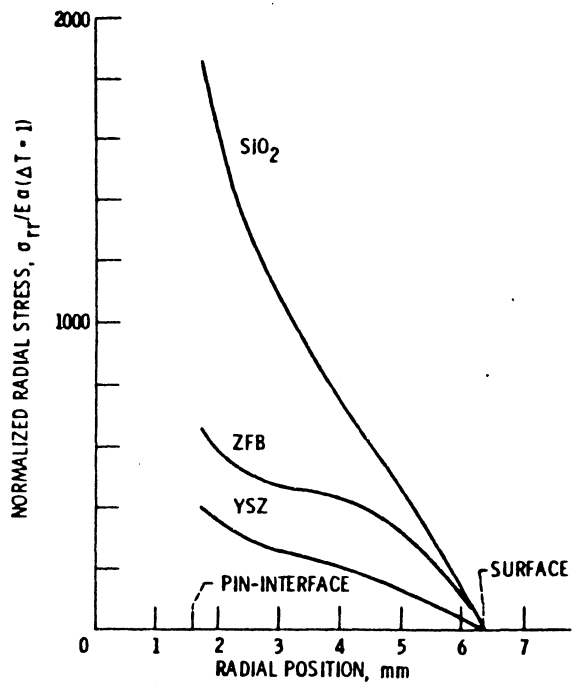

(a) Normalized radial stress.

Figure 2. - Distribution of normalized stress with radial position at 10^{-3} hr into the heating cycle for three thermoprotective materials.

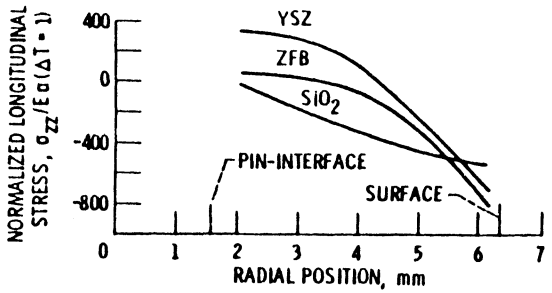

(b) Normalized longitudinal stress.

Figure 2. - Concluded.

1. Report No.	2. Government Accession No.	3. Recipient's Catalog No.
NASA TM-82901		

4. Title and Subtitle	5. Report Date
USE OF FIBER-LIKE MATERIALS TO AUGMENT CYCLE LIFE OF THICK THERMOPROTECTIVE SEAL COATINGS	August 1982
	6. Performing Organization Code 505-32-42
7. Author(s) R. C. Hendricks and G. McDonald	8. Performing Organization Report No. E-1284
	10. Work Unit No.
9. Performing Organization Name and Address National Aeronautics and Space Administration Lewis Research Center Cleveland, Ohio 44135	11. Contract or Grant No.
12. Sponsoring Agency Name and Address National Aeronautics and Space Administration Washington, D. C. 20546	13. Type of Report and Period Covered Technical Memorandum
	14. Sponsoring Agency Code

15. Supplementary Notes

Material previously presented at the International Conference on Metallurgical Coatings and Process Technology sponsored by the American Vacuum Society, San Diego, California, April 4-9, 1982.

16. Abstract

Some experimental and analytical studies of plasma sprayed ZrO_2-Y_2O_3 thick seal thermoprotective materials over NiCrAlY bond coats with testing to 1040° C in a Mach 0.3 burner flame are reviewed. These results indicate the need for material to have both compliance and sufficient strength to function successfully as a thick thermoprotective seal material. Fibrous materials may satisfy many of these requirements. A preliminary analysis simulating the simplified behavior of a 25 mm cylindrical Si02-fiber material indicated significant radial temperature gradients, a relatively cool interface and generally acceptable stresses over the initial portion of the thermal cycle. Subsequent testing of these fiberlike materials in a Mach 0.3 Jet A/air burner flame confirmed these results.

17. Key Words (Suggested by Author(s))	18. Distribution Statement
Seals; Coatings; Fiber materials; Thermoprotective	Unclassified - unlimited STAR Category 34

19. Security Classif. (of this report)	20. Security Classif. (of this page)	21. No. of Pages	22. Price*
Unclassified	Unclassified		

* For sale by the National Technical Information Service, Springfield, Virginia 22161